

# Expression of RASSF6 in kidney and the implication of RASSF6 and the Hippo pathway in the sorbitol-induced apoptosis in renal proximal tubular epithelial cells

Received March 2, 2012; accepted March 21, 2012; published online May 9, 2012

Kanchanamala Withanage<sup>1</sup>,  
Kentaro Nakagawa<sup>1</sup>, Mitsunobu Ikeda<sup>1</sup>,  
Hidetake Kurihara<sup>2</sup>, Takumi Kudo<sup>1,3</sup>,  
Zeyu Yang<sup>1,4</sup>, Ayuko Sakane<sup>5</sup>,  
Takuya Sasaki<sup>5</sup> and Yutaka Hata<sup>1,\*</sup>

<sup>1</sup>Department of Medical Biochemistry, Graduate School of Medicine, Tokyo Medical and Dental University, Tokyo 113-8519; <sup>2</sup>Department of Anatomy, Juntendo University School of Medicine, Tokyo 113-8421; <sup>3</sup>Department of Neurosurgery, Graduate School of Medicine, Tokyo Medical and Dental University, Tokyo 113-8519, Japan; <sup>4</sup>Department of Ultrasound, Shengjing Hospital of China Medical University, Shenyang 110004, China; and <sup>5</sup>Department of Biochemistry, Institute of Health Biosciences, University of Tokushima Graduate School, Tokushima 770-8503, Japan

\*Yutaka Hata, Department of Medical Biochemistry, Graduate School of Medicine, Tokyo Medical and Dental University, 1-5-45 Yushima, Bunkyo-ku, Tokyo 113-8519, Japan.  
Tel: +81-3-5803-5164, Fax: 81-3-5803-0121,  
email: yuhammeh@tmd.ac.jp

**RASSF6, a member of RASSF tumour suppressor proteins, binds to mammalian Ste20-like kinases (MST1/2), core kinases of the proapoptotic Hippo pathway and cooperates with the Hippo pathway to induce apoptosis. We originally identified RASSF6 as a putative interactor of membrane-associated guanylate kinase inverted (MAGI)-1 by the yeast two-hybrid screening. We used human kidney cDNA library for the screening. MAGI-1 is abundantly expressed in kidney and is a core component of the slit diaphragm. These findings suggest that RASSF6 is expressed in kidney. However, the function of RASSF6 in kidney is not yet studied. We performed this study to confirm the interaction of RASSF6 with MAGI-1, to analyse the expression of RASSF6 in kidney and to gain insight into the function of RASSF6 in kidney. RASSF6 binds to PDZ domains of MAGI-1 through its C-terminal PDZ-binding motif and is coimmunoprecipitated with MAGI-1 from rat liver. RASSF6 is localized in normal kidney glomerulus but disappears when the slit diaphragm is disrupted in nephrotic kidney. RASSF6 is also localized on apical membranes in renal proximal tubular epithelial cells. We demonstrated that RASSF6 as well as the Hippo pathway are involved in the sorbitol-induced apoptosis in immortalized human proximal renal tubular epithelial HK-2 cells.**

**Keywords:** apoptosis/Hippo pathway/kidney/RASSF.

**Abbreviations:** DMEM, Dulbecco's Modified Eagle Medium; GST, glutathione *S*-transferase; LATS, large tumour suppressor; MAGI-1, membrane-associated guanylate kinase inverted-1; MBP, maltose-binding protein; MST, mammalian Ste20-like

kinase; PAN, puromycin aminonucleoside; RA, Ras-association; SARAH, Salvador/RASSF/Hippo; TUNEL, terminal deoxynucleotidyl transferase dUTP nick-end labelling.

Human RASSF family is composed of 10 members, RASSF1 to RASSF10 (1–4). RASSF1 to RASSF6 have the Ras-association (RA) domain in the middle region and the Salvador/RASSF/Hippo (SARAH) domain in the C-terminal region. RASSF7 to RASSF10 have the RA domain in the N-terminal region and lack the SARAH domain. The expression of RASSF1A, a splicing variant of RASSF1, is frequently down-regulated in human tumours, and mice lacking RASSF1A are susceptible to carcinogen-induced tumorigenesis. RASSF1A regulates cell cycle and apoptosis. These findings established RASSF1A as a tumour suppressor. RASSF2 to RASSF6 are also regarded as tumour suppressors.

The Hippo pathway regulates cell proliferation and apoptosis (5–8). *Drosophila* C-terminal RASSF, dRASSF, interacts with Hippo kinase and suppresses the Hippo pathway (9). In mammalian cells, RASSF1A and RASSF5 interact with and inhibit Hippo homolog, mammalian Ste20-like kinase (MST) 1, but the coexpression of Ras enhances MST1 activity (10, 11). RASSF1A interacts with MST2 to release it from Raf1-mediated inhibition and enhances MST2 activity to mediate apoptosis through the Hippo pathway (12, 13). RASSF2 and RASSF5 are also reported to activate MST kinases (11, 14, 15). In contrast, RASSF6 inhibits MST1/2 and induces apoptosis independently of the Hippo pathway, and MST kinases reciprocally inhibit RASSF6-mediated apoptosis (16). Based on these findings, we previously proposed the model that RASSF6 and MST1/2 form a complex under the basal condition to inhibit each other and that upon the activation of the Hippo pathway, the complex is dissociated, so that the Hippo pathway and RASSF6-mediated apoptosis are simultaneously activated. As RASSF6 is highly proapoptotic, it is suspected, although not yet examined, that RASSF6 is involved in various pathological conditions (17, 18).

In this study, we demonstrated that endogenous RASSF6 is coimmunoprecipitated with membrane-associated guanylate kinase inverted (MAGI)-1. MAGI-1 is abundant in kidney, directly binds nephrin

and is one of core components of the slit diaphragm (19). MAGI-1 is also localized at tight junctions in polarized epithelial cells (20). We confirmed in immunofluorescence that RASSF6 is expressed in kidney glomeruli but disappears when the slit diaphragm is disrupted as MAGI-1 does. RASSF6 is also detected on apical membranes in proximal tubular epithelial cells. We used immortalized human proximal renal tubular epithelial HK-2 cells to show that RASSF6 and the Hippo pathway play a role in osmotic stress-induced apoptosis in these cells.

## Materials and Methods

### Construction of expression vectors and recombinant proteins

pBTM116 KM MAGI-1, various pGex4T-1 MAGI-1, pCneoGFP-RASSF6 and pMal RASSF6 were described (16, 19, 21). pLenti-EF-ires-blast vector was described (22). pCneoFH-MST2, pCneoFH-NDR1 and pCneoFH-large tumour suppressor (LATS) 2 were digested with *NheI*/*SalI* and the isolated fragments were ligated into *SpeI* and *SalI* sites of pLenti-EF-ires-blast to generate lentivirus vectors for MST2, NDR1 and LATS2. pCneoHA Rab4, pCneoHA Rab5a, pCMV3xFLAG Rab7 and pCneoHA Rab11 were described previously (23–25).

### Antibodies

Rabbit anti-MAGI-1, rabbit phospho-specific NDR1/2, rabbit phospho-specific LATS1/2 and mouse monoclonal anti-RASSF6 (4C2) antibodies were described (17, 20, 26). Rabbit polyclonal anti-RASSF6 antibody was raised against the C-terminal peptide of RASSF6 and affinity-purified. Antibodies and reagents used in this study were obtained from the following sources: mouse anti-Myc 9E10 (American Type Culture Collection); mouse and rabbit anti-FLAG, mouse acetylated-tubulin and mouse anti-HA (Sigma-Aldrich); mouse anti-cytochrome C (BD Pharmingen); mouse anti-GFP (Santa Cruz); rabbit anti-phospho-PAK1 (Cell Signaling) and fluorescein-isothiocyanate, rhodamine- and Cy5-conjugated secondary antibodies (Chemicon International). Phospho-PAK1 (Thr<sup>423</sup>) antibody cross-reacts with phospho-MST1 (Thr<sup>183</sup>) and phospho-MST2 (Thr<sup>180</sup>).

### Yeast two-hybrid screening

Yeast two-hybrid screening was performed using a human kidney cDNA library (Clontech), yeast strain L40 and pBTM116KM MAGI-1 (19).

### Cell culture, transfection and lentivirus production

HK-2 were grown in Dulbecco's Modified Eagle Medium (DMEM)/F12 supplemented with 10% fetal bovine serum, 100 U/ml of penicillin and 100 µg/ml of streptomycin under 5% CO<sub>2</sub> at 37°C, while for HEK293FT cells DMEM was used instead of DMEM/F12. Transfection was performed with Lipofectamine 2000 reagent (Invitrogen). HEK293FT cells were transfected with various pLenti-EF-ires-blast vectors and packaging vectors. Lentivirus was collected from the medium. HK-2 cells were infected with lentivirus and cultured in the medium containing 2 mg/l blasticidin to establish stable transformants.

### RNA interference

HK-2 cells were transfected with 21-nucleotide oligomers (Applied Biosystem) using Lipofectamine RNAiMAX (Invitrogen) to knock-down RASSF6, MST1, MST2, NDR1, NDR2, LATS1 and LATS2. Silencer Negative Control No. 2 (Applied Biosystem) was used as a control. The validity of the knockdown was confirmed by quantitative RT-PCR as described (16). The 21-nucleotide oligomers and the primers for RT-PCR used in this study were described in a previous article (16).

### Apoptosis assays

Terminal deoxynucleotidyl transferase dUTP nick-end labeling (TUNEL) assay was performed using the In Situ Cell Death detection kit (Roche). Caspase-3 activity was measured using

DEVD-MCA (Peptide Institute) as a substrate, and the released MCA was measured (excitation 355 nm and emission 460 nm).

### In vitro interaction assay

Proteins were expressed in HEK293FT cells. Cells from 3.5 cm plates were homogenized in 400 µl of lysis buffer A (25 mM Tris-HCl (pH 7.4), 1 mg/l of 4-aminophenylmethanesulphonyl fluoride, 1 mg/l of leupeptin, 1 mg/l of pepstatin A and 1 mg/l of aprotinin) containing 100 mM NaCl and 1% (w/v) Triton X-100 and centrifuged at 100,000 × *g* for 15 min at 4°C. The supernatant was incubated with anti-FLAG M2 agarose gel (Sigma-Aldrich). The beads were washed three times with 25 mM Tris-HCl (pH 7.4), 100 mM NaCl and 0.33% (w/v) Triton X-100, analysed by SDS-PAGE and immunoblotted with anti-FLAG or anti-Myc antibody.

### RT-PCR for RASSF messages

mRNA was isolated from HK-2 cells using QuickPrep Micro mRNA purification kit (GE Healthcare). Reverse transcription was performed to generate the first-strand cDNA using ImProm-II Reverse Transcription System (Promega). PCR was performed using ExTaq polymerase (Takara). Primers were as follows. RASSF1, 5'-acaagggcactgtgaatcat-3' and 5'-ccttcaggacaagctcagg-3'; RASSF2, 5'-tgccctgtacgtggccata-3' and 5'-ttcccgatcttcttctct-3'; RASSF3, 5'-acaggcagaagctggaagaa-3' and 5'-agaaaggcgaagacctagc-3'; RASSF4, 5'-accgtgaggagaaggact-3' and 5'-ccttagaggcagc taggc-3'; RASSF5 5'-gacactacaacacgcgaga-3' and 5'-aggggcagg tagaaggatgt-3'; and RASSF6, acgtctctccagcaagga-3' and 5'-cag agctgcttactatgg-3'.

### Immunoprecipitation

Rat tissues were homogenized in buffer B (25 mM Tris-HCl (pH 8.0), 100 mM NaCl, 1% (w/v) Triton X-100, 10 mg/l 4-aminophenylmethanesulphonyl fluoride, 10 mg/l leupeptin, 10 mg/l pepstatin A and 10 mg/l aprotinin). The lysates were centrifuged at 100,000 × *g* for 15 min at 4°C. The supernatant was incubated with rabbit anti-MAGI-1 or anti-RASSF6 antibody on 10 µl of protein G Sepharose 4 fast-flow beads (GE Healthcare Bio-Sciences). The beads were washed three times with 25 mM Tris-HCl (pH 8.0), 100 mM NaCl and 0.5% (w/v) Triton X-100. The precipitates were analysed by SDS-PAGE and immunoblotted with mouse anti-RASSF6 or anti-MAGI-1 antibody.

### Pull-down assays

Fifty picomoles of maltose-binding protein (MBP)-RASSF6 was incubated with 10 pmol of glutathione *S*-transferase (GST)-fusion proteins fixed on glutathione-Sepharose 4B beads (GE Healthcare Bio-Sciences) in 500 µl of the buffer B. The precipitates were analysed by SDS-PAGE and immunoblotted with anti-MBP antibody.

### Puromycin aminonucleoside nephropathy

All procedures related to the care and treatment of animals were in accordance with Juntendo University guideline. Young male rats (150 g) were injected intraperitoneally with 10 mg/100 g body weight of puromycin aminonucleoside (PAN; Sigma-Aldrich). Animals were killed on day 11 for immunofluorescence study.

### Immunofluorescence microscopy

Immunofluorescence studies were performed as described (19).

### Statistical analysis

Statistical analyses were performed using ANOVA with Bonferroni *post hoc* test for multiple comparisons by GraphPad Prism software (GraphPad Software). Data expressed as percentages were subjected to arcsine square root transformation before Student's *t*-test or ANOVA.

## Results

### RASSF6 interacts with MAGI-1

Allen *et al.* (18) reported that the message of RASSF6 is abundant in colon, kidney, placenta and thymus. To evaluate RASSF6 protein expression, we raised a

rabbit antibody against the C-terminus of RASSF6. We first immunoprecipitated RASSF6 from rat tissues with this rabbit antiserum to enrich RASSF6 and then immunoblotted the precipitates with mouse monoclonal antibody. RASSF6 protein was detected in lung, liver, kidney, stomach, thymus and spleen (Fig. 1A). We originally obtained RASSF6 as a candidate MAGI-1-interacting protein through the yeast two-hybrid screening using human kidney cDNA library. To confirm the coimmunoprecipitation of endogenous RASSF6 and MAGI-1, we used rat liver lysates, because RASSF6 is abundant in liver and MAGI-1 is resistant to the solubilization from rat kidney (19). RASSF6 was coimmunoprecipitated with MAGI-1 (Fig. 1B). In heterologous HEK293FT cells, the full-length RASSF6 was coimmunoprecipitated with MAGI-1, whereas the deletion mutant lacking the C-terminal PDZ-binding motif was not (Fig. 1C). MAGI-1 harbours five typical PDZ domains (PDZ1 to PDZ5) in addition to the N-terminal PDZ-like domain (PDZ0). MBP-RASSF6 bound GST proteins harbouring the third and the fourth PDZ domains (PDZ2 and PDZ3) (Fig. 1D). All these findings support the RASSF6 directly binds to the PDZ domains of MAGI-1.

**RASSF6 is detected in the kidney glomerulus and in proximal tubular epithelial cells**

We immunostained rat kidney with the purified rabbit RASSF6 antibody. RASSF6 was detected in the

glomerulus and was overlapped with ZO-1 (Fig. 2A, the upper panel and arrow heads). In PAN-treated nephrotic kidney, RASSF6 signals in the glomerulus decreased, but ZO-1 signals remained (Fig. 2B, the upper panel). This finding suggests that RASSF6 is associated with the slit diaphragm like MAGI-1. RASSF6 was also detected in the proximal tubular epithelial cells (Fig. 2A, the lower panel). RASSF6 was concentrated on apical membranes, where it was colocalized with megalin signal (arrows), but was also diffusely detected in cytoplasm. In PAN-treated kidney, RASSF6 translocated to the endocytotic vacuoles in the proximal tubular epithelial cells (Fig. 2B, the lower panel and arrows).

**The messages of RASSF1 to RASSF6 are detected in HK-2 cells**

RASSF6 is involved in apoptosis in various cells, although the underlying molecular mechanism is unclear (16–18). The high expression of RASSF6 in renal proximal tubular epithelial cells prompted us to examine whether RASSF6 plays a role in apoptosis in these cells. To test this idea, we used immortalized human proximal tubular epithelial HK-2 cells, because we knew that human RASSF6 is well suppressed by our knockdowns. We first confirmed the expression of RASSF6 in these cells. As our anti-RASSF6 antibody does not recognize human RASSF6 efficiently, we performed RT-PCR for the C-terminal RASSF

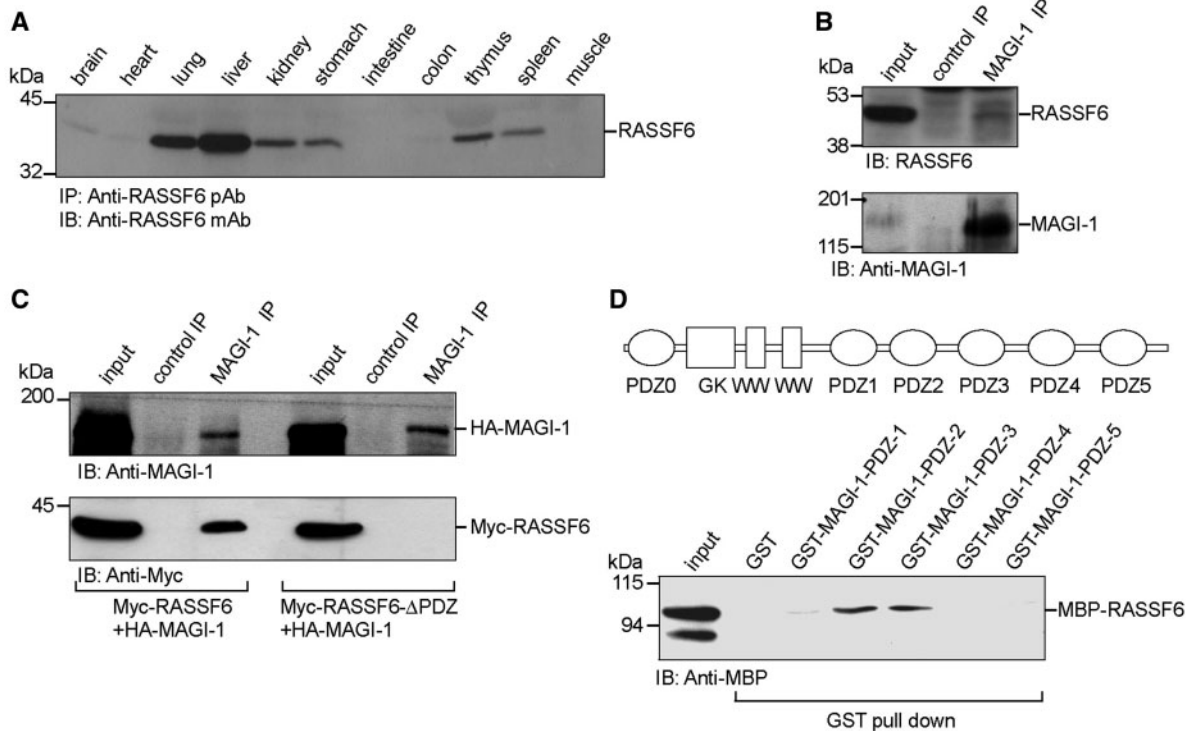


**Fig. 1 Interaction between RASSF6 and MAGI-1.** (A) RASSF6 was immunoprecipitated from lysates (total protein of 1 mg) of rat tissues with rabbit anti-RASSF6 antiserum. The immunoprecipitates were immunoblotted with mouse anti-RASSF6 antibody. (B) MAGI-1 was immunoprecipitated from rat liver lysates. The immunoprecipitates were immunoblotted with anti-RASSF6 and anti-MAGI-1 antibodies. (C) HA-MAGI-1 was expressed with Myc-RASSF6 or Myc-RASSF6 mutant lacking the C-terminal PDZ-binding motif (Myc-RASSF6-ΔPDZ). The immunoprecipitation was performed with control serum or anti-MAGI-1 antibody. The immunoprecipitates were immunoblotted with anti-HA or anti-Myc antibody. (D) 50 pmol of purified MBP-RASSF6 was pulled down with 10 pmol of either control GST or GST-MAGI-1 proteins covering indicated PDZ domains.

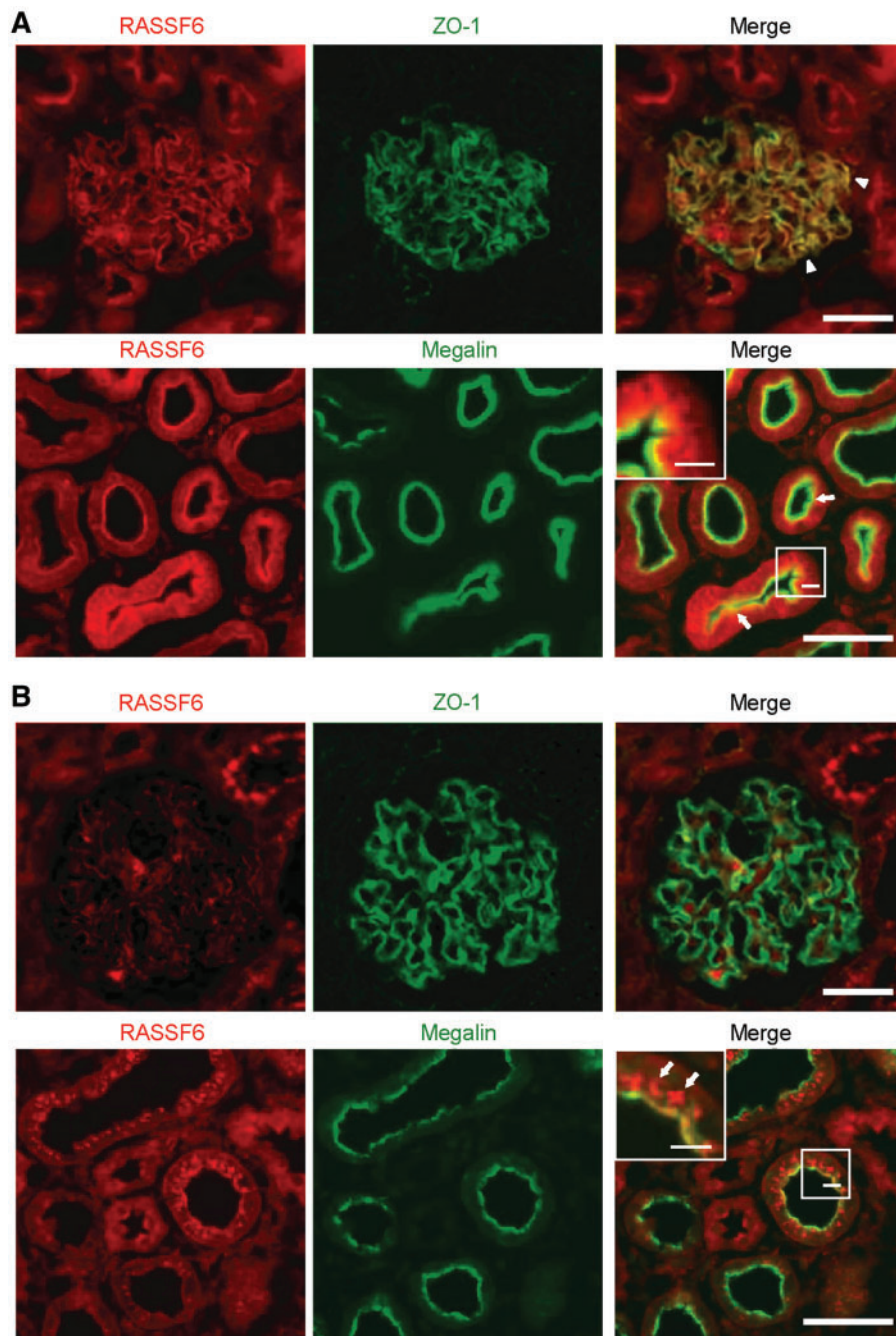


**Fig. 2 RASSF6 in rat kidney.** (A) RASSF6 in intact rat kidney. RASSF6 is detected in the glomerulus (the upper panel) and on apical membranes in renal proximal tubular epithelial cells (the lower panel, arrows). The inset shows the marked area at higher magnification. (B) RASSF6 in PAN-induced nephrotic kidney. RASSF6 signals disappear from the glomerulus, whereas ZO-1 signals remain (the upper panel). RASSF6 is accumulated to vacuole-like structures in proximal tubular epithelial cells (the lower panel). The inset shows the marked area at higher magnification. Arrows show the accumulation of RASSF6 to the vacuole-like structures. Bar, 100  $\mu\text{m}$ . Bar in the inset, 20  $\mu\text{m}$ .

proteins. The messages of all the C-terminal RASSFs were detected in HK-2 cells (Fig. 3).

#### **Sorbitol treatment induces apoptosis in HK-2 cells**

RASSF6 interacts with MST1/2 and is closely related with the Hippo pathway. We proposed that the Hippo pathway and RASSF6 simultaneously but independently mediate apoptosis in HeLa cells and rat hepatocytes (16). Therefore, we examined whether not only

RASSF6 but also the Hippo pathway are involved in apoptosis in HK-2 cells. It is not yet clarified whether MST1/2 are activated by osmotic stress, but other Ste20-like kinases are reported to be activated by osmotic shock (27). Therefore, we attempted to induce apoptosis in HK-2 cells with the high osmolarity. When exposed to 500 mM sorbitol, HK-2 cells exhibited nuclear condensation (Fig. 4A). TUNEL-positive cells increased (Fig. 4B). Caspase-3 cleavage

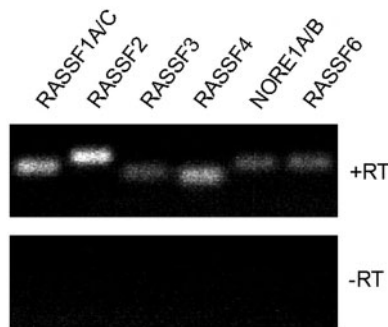


**Fig. 3** The messages of the C-terminal RASSF proteins in immortalized human renal proximal tubular epithelial cells. mRNA was isolated from HK-2 cells and RT-PCR was performed with (the upper panel, +RT) or without (the lower panel, -RT) the reverse transcriptase to detect the messages of RASSF1 to RASSF6 in HK-2 cells.

was detected (Fig. 4C). These findings indicate that the sorbitol treatment induces apoptosis in HK-2 cells.

#### **Sorbitol treatment activates the Hippo pathway**

We subsequently examined whether the sorbitol treatment activates the Hippo pathway in HK-2 cells. The phosphorylations of MST2 and LATS2 are the hallmarks of the activation of the pathway. NDR1 is also activated by MST2. However, the antibodies against the phosphorylated-MST2, -NDR1 and -LATS2 are not sensitive enough to detect the phosphorylation of endogenous kinases. Hence, we generated HK-2 cells stably expressing MST2, NDR1 or LATS2 and treated these cells with 500 mM sorbitol to use for the evaluation of the Hippo pathway activation. The sorbitol treatment induced the phosphorylation of all these kinases, supporting the activation of the Hippo pathway (Fig. 5A).

#### **The Hippo pathway and RASSF6 are both involved in the sorbitol-induced apoptosis of HK-2 cells**

We next suppressed NDR1/2 and LATS1/2 in HK-2 cells with RNA interference. LATS1/2 knockdown decreased the number of TUNEL-positive cells and the caspase-3 activation, but NDR1/2 knockdown had no effect (Fig. 5B). The data suggest that although NDR1 and NDR2 are involved in Fas-promoted apoptosis in HeLa cells, they are not important for the sorbitol-induced apoptosis in HK-2 cells (28). According to our previous study, when the Hippo pathway is activated, RASSF6 should induce apoptosis in the Hippo pathway-independent manner. Consistently, the knockdown of RASSF6 partially but significantly suppressed the increase of TUNEL-positive cells and the caspase-3 activation (Fig. 5B and C). In contrast, the knockdown of MST1/2 had no effect on apoptosis. This paradoxical observation is consistent with that MST1/2 inhibits RASSF6-induced apoptosis and that RASSF6 makes more contributions to apoptosis than the Hippo pathway itself.

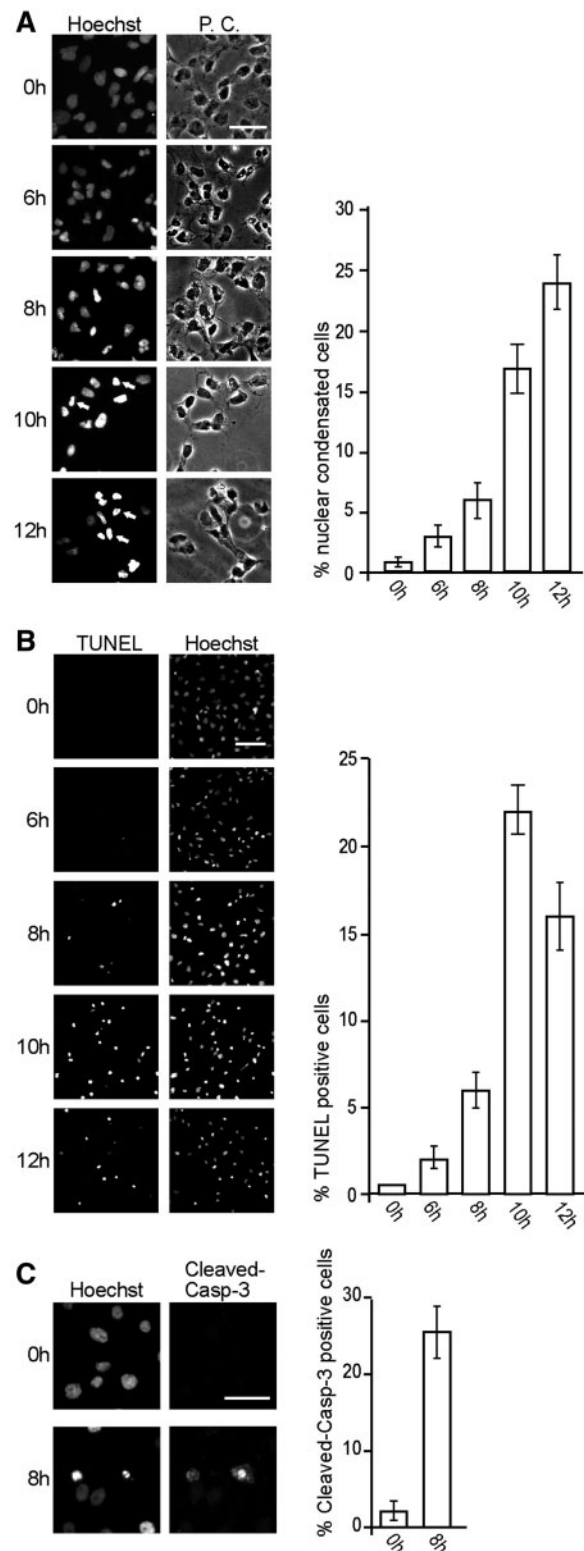


**Fig. 4** Apoptosis in the sorbitol-treated HK-2 cells. HK-2 cells were exposed to 500 mM sorbitol. The nuclear condensation (A) and TUNEL assay-positive cells (B) were evaluated. P.C. phase contrast the cells in five fields (more than 50 cells) were analysed for each experiment. The data represent three independent experiments. (C) The cells were immunostained with anti-cleaved caspase-3 antibody. The cells in five independent fields (20–30 cells) were analysed for quantification. Bars 50  $\mu$ m in (A) and (C); and 100  $\mu$ m in (B).

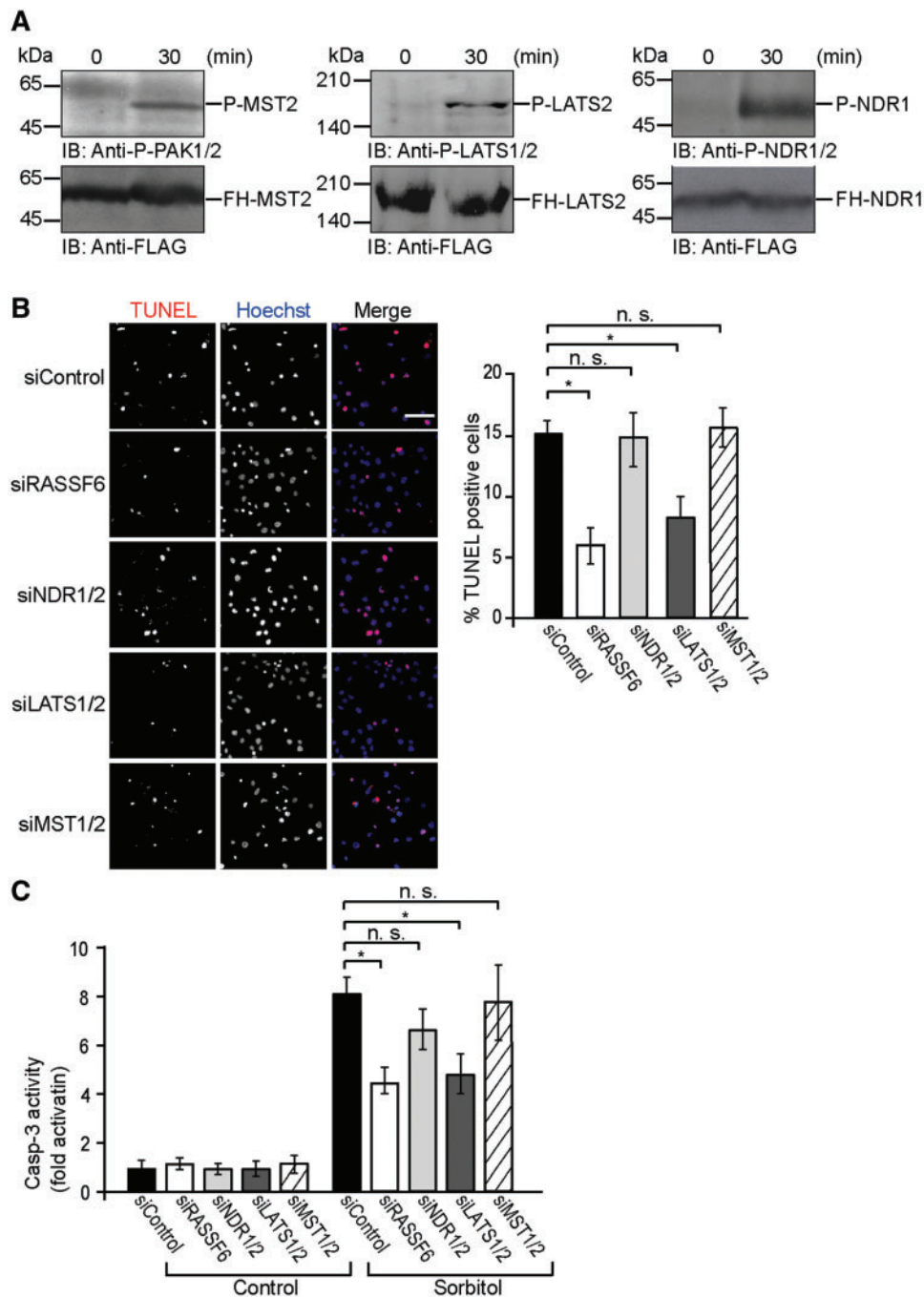


**Fig. 5** Implication of RASSF6 and the Hippo pathway in the sorbitol-induced apoptosis in HK-2 cells. (A) HK-2 cells expressing FLAG-MST2 (FH-MST2), -LATS2 (FH-LATS2), and -NDR1 (FH-NDR1) were exposed to 500 mM sorbitol. The cells were harvested at 0 and 30 min, and were immunoblotted with either the phosphorylation-specific antibodies (the upper panels) or anti-FLAG-antibody (the lower panels). In (B) and (C) RASS6, MST1/2, LATS1/2 and NDR1/2 were knocked down in HK-2 cells before the exposure to 500 mM sorbitol. (B) Apoptosis was evaluated with the TUNEL assay as described for Fig. 3. (C) Caspase-3 activity was measured using DEVD-MCA as a substrate. Error bars indicate SD of three independent experiments. \* $P < 0.05$ . n.s., not significant.

#### **RASSF6 is accumulated to the Rab11-positive compartment in response to the sorbitol treatment**

During this study, we found that RASSF6 changes its subcellular localization in HK-2 cells in response to the sorbitol treatment. GFP-RASSF6 formed clusters at 30 min after the exposure to 500 mM sorbitol and was subsequently accumulated to the perinuclear regions (Fig. 6A). To identify the compartment

where RASS6 was accumulated, we coexpressed GFP-RASSF6 with various Rab proteins as markers. GFP-RASSF6 was not colocalized with Rab5a or Rab7 (Fig. 6B). RASSF6 was partially overlapped with Rab4, and the perinuclear RASSF6 remarkably colocalized to Rab11 (Fig. 6B). We also circumstantially observed the localization of GFP-RASSF6 to the basal portion of the primary cilia (Fig. 6C).

## Discussion

We obtained RASSF6 as a putative MAGI-1-interactor in the yeast two-hybrid screening. Endogenous RASSF6 and MAGI-1 are coimmunoprecipitated from rat liver. RASSF6 binds to PDZ domains of MAGI-1 through its C-terminal PDZ-binding motif in heterologous cells. RASSF6 is detected in the glomerulus in rat kidney, but disappears in PAN-treated kidney in a similar manner to core components of the slit diaphragm such as MAGI-1 and nephrin (19). ZO-1 is accumulated in the occluding type junctions and is detectable even in PAN-induced nephrotic glomerulus. These findings suggest that RASSF6 behaves more similarly to MAGI-1 than to ZO-1 and that the localization of RASSF6 in the glomerulus is closely related to the slit diaphragm. RASSF6 is additionally detected on apical membranes in proximal renal tubular epithelial cells and is colocalized with megalin. We previously reported that MAGI-1 is detected at tight junctions, but not on apical membranes, in the polarized epithelial cells such as intestinal epithelial and Madin-Darby canine kidney II cells (20). According to our previous report, it follows that RASSF6 is not colocalized with MAGI-1 in the proximal renal tubular epithelial cells. However, we need to consider that MAGI-1 has splicing variants and that our antibody reacts with the N-terminal region of MAGI-1 (29). A previous article reports that MAGI-1 interacts with megalin (30). As megalin is localized on apical membranes, some MAGI-1 variant may be localized on apical membranes and interacts with RASSF6. If this is the case, as megalin binds to PDZ5 of MAGI-1, which is different from RASSF6-binding PDZ domains, MAGI-1 may function as a scaffold to link megalin and RASSF6.

It has been reported that MAGI-1 is cleaved by caspases in Fas-treated 3T3 A31 cells and UV-irradiated HaCaT cells and that this cleavage is important for apoptosis (31). It is tempting to speculate that RASSF6 is implicated in this MAGI-1-mediated apoptosis. We tested the effect of MAGI-1 on RASSF6-induced apoptosis using HeLa cells. Contrary to our expectations, neither overexpression nor knockdown of MAGI-1 showed any effect (data not shown). It may be necessary using other cells, *e.g.* 3T3 A31 cells, HaCaT cells or podocytes, to examine whether MAGI-1-induced apoptosis and RASSF6-induced apoptosis are related to each other.

Although the underlying molecular mechanism is not yet fully clear, RASSF6 mediates apoptosis. RASSF6 expression induces apoptosis in various cells in caspase-dependent and -independent manners (17, 18). Its depletion blocks tumour necrosis factor- $\alpha$ - and okadaic acid-induced apoptosis in HeLa cells and rat hepatocytes. As RASSF6 is highly expressed in proximal tubular epithelial cells in rat kidney, we hypothesized that RASSF6 plays a role in apoptosis in these cells. Based on our previous findings that RASSF6 and the Hippo pathway cooperate to induce apoptosis, we speculated that the Hippo pathway is as well involved in apoptosis in these

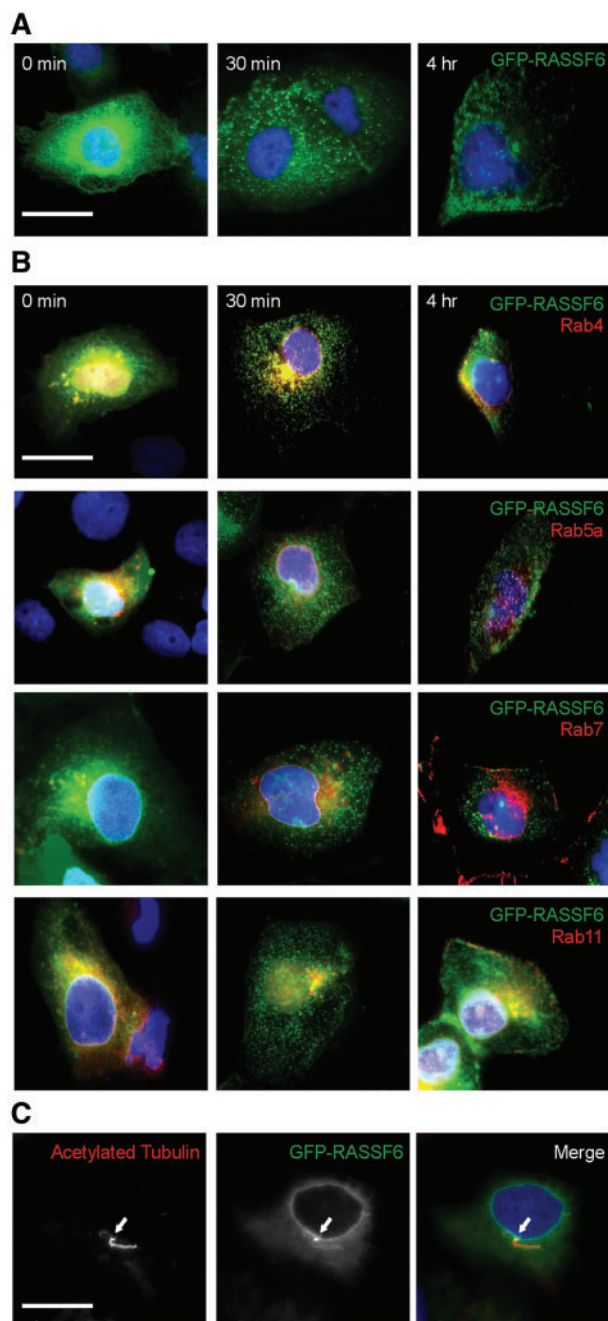


**Fig. 6** The subcellular localization of GFP-RASSF6 in HK-2 cells. (A) HK-2 cells transiently expressing GFP-RASSF6 was exposed to 500 mM sorbitol. The cells were fixed and immunostained at the indicated time points. (B) HK-2 cells were transfected with pCneoGFP RASSF6 and various Rab constructs (HA-Rab4, HA-Rab5a, FLAG-Rab7 and HA-Rab11) and exposed to 500 mM sorbitol. The cells were fixed and immunostained at the indicated time points. (C) HK-2 cells expressing GFP-RASSF6 were grown to confluency, cultured with the serum-starved medium for 48 h and immunostained with anti-acetylated tubulin antibody to detect the primary cilia.

cells. To test this idea, we used HK-2 cells and exposed the cells to the high concentration of sorbitol, because it is reported for Ste20-like kinases other than MST1/2 to be activated by osmotic shock (27). As expected, MST2, NDR1 and LATS2 were activated in sorbitol-treated HK-2 cells. The knockdown of

LATS1/2 suppressed the sorbitol-induced apoptosis, indicating that the Hippo pathway contributes to apoptosis. Importantly, these observations indicate that osmotic stress activates MST1/2 as well as other Ste20-like kinases and eventually the Hippo pathway. RASSF6 depletion partially but significantly attenuated sorbitol-induced apoptosis. As MST1/2 are key activators of LATS1/2, their knockdown should block apoptosis, but had no effect. We obtained a similar paradoxical result from okadaic acid-treated rat hepatocytes (16). In those cells, MST1/2 depletion rather enhanced apoptosis, whereas RASSF6 depletion reduced it. These findings are comprehensible, taking into consideration the bidirectional effect of MST1/2, which mediate the proapoptotic Hippo pathway through the activation of LATS1/2 and inhibit the Hippo-independent RASSF6-induced apoptosis.

During this study, we incidentally found that in HK-2 cells, RASSF6 changes its subcellular localization in response to the sorbitol treatment. The colocalization of RASSF6 with Rab4 and Rab11 suggests the implication of RASSF6 in the specific plasma membrane recycling events, which both Rab4 and Rab11 are involved in (32). Rab11 is also required for cell division and is involved in the activation of Rab8, which is essential for the cilia formation (33, 34). Therefore, given the localization of GFP-RASSF6 to the basal portion of the primary cilia, RASSF6 may play some role in the primary cilia. The meanings of the characteristic subcellular localization of RASSF6 need to be clarified in the future studies.

We launched this study to confirm the interaction of RASSF6 with MAGI-1, to analyse the expression of RASSF6 in kidney and to gain insight into the function of RASSF6 in kidney. In conclusion, we confirmed that RASS6 is a *bona fide* interactor with MAGI-1. We revealed the association of RASSF6 with the slit diaphragm and its expression in renal proximal tubular epithelial cells. We also demonstrated that RASSF6 and the Hippo pathway play roles in the sorbitol-induced apoptosis in HK-2 cells. All these findings suggest that RASSF6 and the Hippo pathway are implicated in the pathological conditions, such as contrast-induced nephropathy, under which proximal tubular epithelial cells are exposed to high osmolarity.

## Acknowledgements

The authors thank Dr Masaomi Nangaku (The University of Tokyo) for HK-2 cells.

## Funding

Japan Society for the Promotion of Science (JSPS) (22790275 and 22590267), Takeda Science Foundation, Suzuken Memorial Foundation and the Nakatomi Foundation, TAKASE Foundation Scholarship (to K.W.) and Japanese Government (Monbukagakusho) scholarship (to Z.Y.).

## Conflict of interest

None declared.

## References

- Avruch, J., Xavier, R., Bardeesy, N., Zhang, X.F., Praskova, M., Zhou, D., and Xia, F. (2009) RASSF family of tumor suppressor polypeptides. *J. Biol. Chem.* **284**, 11001–11005
- Richter, A.M., Pfeifer, G.P., and Dammann, R.H. (2009) The RASSF proteins in cancer; from epigenetic silencing to functional characterization. *Biochim. Biophys. Acta* **1796**, 114–128
- Sherwood, V., Recino, A., Jeffries, A., Ward, A., and Chalmers, A.D. (2009) The N-terminal RASSF family: a new group of Ras-association-domain-containing proteins, with emerging links to cancer formation. *Biochem. J.* **425**, 303–311
- Underhill-Day, N., Hill, V., and Latif, F. (2011) N-terminal RASSF family: RASSF7-RASSF10. *Epigenetics* **6**, 284–292
- Bao, Y., Hata, Y., Ikeda, M., and Withanage, K. (2011) Mammalian Hippo pathway: from development to cancer and beyond. *J. Biochem.* **149**, 361–379
- Pan, D. (2010) The hippo signaling pathway in development and cancer. *Dev. Cell* **19**, 491–505
- Zhao, B., Tumaneng, K., and Guan, K.L. (2011) The Hippo pathway in organ size control, tissue regeneration and stem cell self-renewal. *Nat. Cell Biol.* **13**, 877–883
- Chan, S.W., Lim, C.J., Chen, L., Chong, Y.F., Huang, C., Song, H., and Hong, W. (2011) The Hippo pathway in biological control and cancer development. *J. Cell. Physiol.* **226**, 928–939
- Polesello, C., Huelsmann, S., Brown, N.H., and Tapon, N. (2006) The *Drosophila* RASSF homolog antagonizes the Hippo pathway. *Curr. Biol.* **16**, 2459–2465
- Khokhlatchev, A., Rabizadeh, S., Xavier, R., Nedwidek, M., Chen, T., Zhang, X.F., Seed, B., and Avruch, J. (2002) Identification of a novel Ras-regulated proapoptotic pathway. *Curr. Biol.* **12**, 253–265
- Praskova, M., Khokhlatchev, A., Ortiz-Vega, S., and Avruch, J. (2004) Regulation of the MST1 kinase by autophosphorylation, by the growth inhibitory proteins, RASSF1 and NORE1, and by Ras. *Biochem. J.* **381** (Pt2), 453–462
- Matallanas, D., Romano, D., Yee, K., Meissl, K., Kucerova, L., Piazzolla, D., Baccarini, M., Vass, J.K., Kolch, W., and O'Neill, E. (2007) RASSF1A elicits apoptosis through an MST2 pathway directing proapoptotic transcription by the p73 tumor suppressor protein. *Mol. Cell* **27**, 962–975
- Guo, C., Tommasi, S., Liu, L., Yee, J.K., Dammann, R., and Pfeifer, G.P. (2007) RASSF1A is part of a complex similar to the *Drosophila* Hippo/Salvador/Lats tumor-suppressor network. *Curr. Biol.* **17**, 700–705
- Cooper, W.N., Hesson, L.B., Matallanas, D., Dallol, A., von Kriegsheim, A., Ward, R., Kolch, W., and Latif, F. (2009) RASSF2 associates with and stabilizes the proapoptotic kinase MST2. *Oncogene* **28**, 2988–2998
- Song, H., Oh, S., Oh, H.J., and Lim, D.S. (2010) Role of the tumor suppressor RASSF2 in regulation of MST1 kinase activity. *Biochem. Biophys. Res. Commun.* **391**, 969–973
- Ikeda, M., Kawata, A., Nishikawa, M., Tateishi, Y., Yamaguchi, M., Nakagawa, K., Hirabayashi, S., Bao, Y., Hidaka, S., Hirata, Y., and Hata, Y. (2009) Hippo pathway-dependent and -independent roles of RASSF6. *Sci. Signal.* **2**, ra59



17. Ikeda, M., Hirabayashi, S., Fujiwara, N., Mori, H., Kawata, A., Iida, J., Bao, Y., Sato, Y., Iida, T., Sugimura, H., and Hata, Y. (2007) Ras-association domain family protein 6 induces apoptosis *via* both caspase-dependent and caspase-independent pathways. *Exp. Cell Res.* **313**, 1484–1495
18. Allen, N.P., Donniger, H., Vos, M.D., Eckfeld, K., Hesson, L., Gordon, L., Birrer, M.J., Latif, F., and Clark, G.J. (2007) RASSF6 is a novel member of the RASSF family of tumor suppressors. *Oncogene* **26**, 6203–6211
19. Hirabayashi, S., Mori, H., Kansaku, A., Kurihara, H., Sakai, T., Shimizu, F., Kawachi, H., and Hata, Y. (2005) MAGI-1 is a component of the glomerular slit diaphragm that is tightly associated with nephrin. *Lab. Invest.* **85**, 1528–1543
20. Ide, N., Hata, Y., Nishioka, H., Hirao, K., Yao, I., Deguchi, M., Mizoguchi, A., Nishimori, H., Tokino, T., Nakamura, Y., and Takai, Y. (1999) Localization of membrane-associated guanylate kinase (MAGI)-1/BAI-associated protein (BAP)1 at tight junctions of epithelial cells. *Oncogene* **18**, 7810–7815
21. Ohno, H., Hirabayashi, S., Kansaku, A., Yao, I., Tajima, M., Nishimura, W., Ohnishi, H., Mashima, H., Fujita, T., Omata, M., and Hata, Y. (2003) Carom: a novel membrane-associated guanylate kinase-interacting protein with two SH3 domains. *Oncogene* **22**, 8422–8431
22. Bao, Y., Nakagawa, K., Yang, Z., Ikeda, M., Withanage, K., Ishigami-Yuasa, M., Okuno, Y., Hata, S., Nishina, H., and Hata, Y. (2011) A cell-based assay to screen stimulators of the Hippo pathway reveals the inhibitory effect of dobutamine of the YAP-dependent gene transcription. *J. Biochem.* **150**, 199–208
23. Mizuno, K., Kitamura, A., and Sasaki, T. (2003) Rabring7, a novel Rab7 target protein with a RING finger motif. *Mol. Biol. Cell* **14**, 3741–3752
24. Terai, T., Nishimura, N., Kanda, I., Yasui, N., and Sasaki, T. (2006) JRAB/MICAL-L2 is a junctional Rab13-binding protein mediating the endocytic recycling of occludin. *Mol. Biol. Cell* **17**, 2465–2475
25. Yamaura, R., Nishimura, N., Nakatsuji, H., Arase, S., and Sasaki, T. (2008) The interaction of JRAB/MICAL-L2 with Rab8 and Rab13 coordinates the assembly of tight junctions and adherens junctions. *Mol. Biol. Cell* **19**, 971–983
26. Bao, Y., Sumita, K., Kudo, T., Withanage, K., Nakagawa, K., Ikeda, M., Ohno, K., Wang, Y., and Hata, Y. (2009) Roles of mammalian sterile 20-like kinase 2-dependent phosphorylations of Mps one binder 1B in the activation of nuclear Dbf2-related kinases. *Genes Cells* **14**, 1369–1381
27. Delpire, E. (2009) The mammalian family of sterile 20 p-like protein kinases. *Pflugers Arch.* **458**, 953–967
28. Vichalkovski, A., Gresko, E., Cornils, H., Hergovich, A., Schmitz, D., and Hemmings, B.A. (2008) NDR kinase is activated by RASSF1A/MST1 in response to Fas receptor stimulation and promotes apoptosis. *Curr. Biol.* **18**, 1889–1895
29. Laura, R.P., Ross, S., Koeppen, H., and Lasky, L.A. (2002) MAGI-1: a widely expressed, alternatively spliced tight junction protein. *Exp. Cell Res.* **275**, 155–170
30. Patrie, K.M., Drescher, A.J., Goyal, M., Wiggins, R.C., and Margolis, B. (2001) The membrane-associated guanylate kinase protein MAGI-1 binds megalin and is present in glomerular podocytes. *J. Am. Soc. Nephrol.* **12**, 667–677
31. Gregorc, U., Ivanova, S., Thomas, M., Guccione, E., Glaunsinger, B., Javier, R., Turk, V., Banks, L., and Turk, B. (2007) Cleavage of MAGI-1, a tight junction PDZ protein, by caspases is an important step for cell–cell detachment in apoptosis. *Apoptosis* **12**, 343–354
32. Scita, G. and Fiore, P.P. (2010) The endocytic matrix. *Nature* **463**, 464–473
33. Horgan, C.P. and McCaffrey, M.W. (2009) The dynamic Rab11-FIPs. *Biochem. Soc. Trans.* **37**, 1032–1036
34. Fürthauer, M. and González-Gaitán, M. (2009) Endocytosis and mitosis: a two way relationship. *Cell Cycle* **8**, 3311–3318